Spontaneous Spatial Alignment of Polymer Cylindrical Nanodomains on Silicon Nitride Gratings

Deepak Sundrani and S. J. Sibener*

The James Franck Institute and the Department of Chemistry, The University of Chicago, 5640 South Ellis Avenue, Chicago, Illinois 60637

Received May 1, 2002

ABSTRACT: We report a simple method to align lying-down cylindrical domains of PS-*b*-PMMA in the trough regions of 555 nm deep silicon nitride gratings without the aid of an external orientation field. This alignment is perpendicular to the orientation of the grating lines and essentially spans the width of the grating trough. The proposed mechanism involves polymer flow and confinement in small dimensions. Also, regularly spaced bumps of almost uniform size can be formed on the crest regions of the support grating. The thickness dependence of PS-*b*-PMMA thin film surface morphology is also utilized to generate micron-scale periodic structures on 115 nm deep gratings. These experiments to align microdomains with controlled nanometer-scale spacing can be extended to generate self-organizing nanofabricated surfaces.

Introduction

Diblock copolymers, composed of two unlike chains joined end-to-end by a single covalent bond, undergo microphase separation to form periodic nanometer scale domains.[1] If the block lengths are very different, the domains take the form of cylinders or spheres of the minority component embedded in a matrix of the majority component. Thin films of such polymers show novel behavior not found in bulk materials because, as the film thickness decreases, the influence of the interfaces at either film surface becomes more prominent; the strong substrate interactions and presence of such interfaces can lead to morphologies that are unique to thin films.[2−4]

Asymmetric diblocks are good candidates for use as nanolithographic[5,6] templates because two-dimensional periodic patterns can be produced with either a monolayer film of close-packed spheres or a thin film containing an array of cylinders oriented parallel or perpendicular to the film plane. The size and separation of the domains are typically 10−50 nm; the domain patterns are self-assembling, enabling parallel processing of large areas. The experimental control of perfection in the resulting nanostructure of diblock copolymers is important in realizing their application for electron transport in confined and periodic geometries. The selective decoration[7] of individual diblock components with either conductive or magnetic nanoparticles in such aligned structures can lead to the generation of electronic and magnetic nanostructures useful for magnetic storage applications. The presence of topological defects such as dislocations and disclinations[8−12] limits the persistence length of these spontaneously formed microdomains which, in turn, make it difficult to use these materials for such applications.

The surface structure and alignment of nanodomains in block copolymers have been studied extensively in bulk,[13−16] solution,[17] and thin films[18−25] on flat, i.e., smooth, substrates. Various strategies such as external electric field,[13,15,17,19,20] copolymer−substrate interaction,[22−25] shear field,[14] solvent vapor treatment,[21] annuli formation,[18] and temperature gradient[16] have resulted in the alignment of block copolymer domains. Recently, some theoretical and experimental work has been done to study the behavior of polymer thin films on substrates imparted with chemical or topographic patterns. By using such substrates, film surface morphology, local domain orientation, and long-range order can be affected and controlled.

In this paper, we will present a new, efficient method for preparing aligned block copolymer structures of unusual geometry on corrugated substrates. But first, let us review the relevant prior theoretical and experimental work in this field.

Theoretical treatments[26−30] of diblock copolymer films deposited onto chemically heterogeneous surfaces generally discern the effect of substrate pattern periodicity on polymer film morphology. When the period of the substrate pattern approaches molecular dimensions, all studies have predicted a surface-perpendicular orientation of lamellar block copolymer domains. The experimental work[30−33] has supported these predictions.

Patterned surface topography[30,34−41] offers another means of controlling polymer surface structure. For relatively shallow height corrugation it has been observed that thin polystyrene (PS) films prepared on regularly corrugated silicon substrates (peak-to-valley depth of 5 nm) are unstable and dewet when the thickness of the film is below a critical limit. Here the dewetting process leads to the formation of nanoscale PS channels which fill the grooves of the corrugated substrates. Films thicker than the critical thickness appear stable and follow the underlying corrugation pattern. This critical thickness was found to scale with the radius of gyration of the unperturbed polymer chains.[38] Turner et al.[35] have performed theoretical studies on the behavior of diblock lamellar layers in the melt, assembled at a substrate with a small-amplitude periodic roughness. They discussed the in-phase or out-of-phase undulation of the free polymer surface with respect to the substrate surface and the penetration of the undulation induced by the substrate into the lamellar stack. Morphology of symmetric diblock copolymer films, which have a film thickness smaller than the bulk

* To whom correspondence should be addressed. E-mail: s-sibener@uchicago.edu.

10.1021/ma020674p CCC: $22.00
Published on Web 09/24/2002

equilibrium period, has also been studied numerically[34] on corrugated substrates. The results show that the formation of uniformly sized lateral domains that appear randomly on a flat surface can be controlled by using topographically patterned substrates. Control of the lateral pattern fails if the distance between the steps of the substrate is smaller than the bulk lamellar wavelength or if the lateral size of the corrugation is larger than the bulk lamellar wavelength.

Fasolka et al.[39] have experimentally studied the morphology of symmetric diblock copolymer films having thickness below the bulk equilibrium period supported by corrugated silicon substrates. Here the uniformly sized lateral domains, which arrange randomly on flat silicon substrates, were observed to decorate the peaks of the substrate corrugation. Micron-scale periodic structures[37] have also been generated by directional solidification of cylinder forming block copolymer using directionally crystallizing solvent (benzoic acid) on a topographically patterned silicon substrate. The substrate features shape the film morphology by periodically modulating the local film thickness, which results in the periodic structure consisting of in-plane and vertically aligned cylindrical domains. Segalman et al.[36] have demonstrated that graphoepitaxy, using patterned silicon substrates, offers a simple method to produce thin film arrays of spherical block copolymer domains with long-range order. Li et al.[40,41] have conducted experiments on thin films of copolymer PS-*b*-P2VP on periodic silicon gratings and observed that the critical height of the surface grating, which is defined by the transition from conformal behavior to the anticonformal conformation, is proportional to the lamellar height of the diblock copolymer. Diblock copolymer films were also observed to propagate substrate roughness over significantly larger distances than observed for amorphous homopolymers.

Previously, in our group, Hahm et al.[18] introduced a simple spin-casting method which produced annular structures on silicon oxide substrates from cylinder-forming PS-*b*-PMMA. The cylinders exhibited a high degree of long-range, i.e., micron-length, microdomain spatial coherence with alignment perpendicular to the rims of the annuli. Radial alignment of microdomains in nL thick films (where n is an integer and L is the natural thickness of one layer of cylinders) was achieved without the application of any externally applied guiding fields. The microdomain alignment spread out radially up to 2 μm in length and was oriented perpendicularly to the step boundaries which separated the different film thickness regions in the annular rim. The extended length of aligned microdomains was limited by annuli step width; i.e., high aspect ratio structures were routinely generated having nanoscale alignment over microns. The confinement of cylinders in nL thick regions between the steps and the flow of the diblock copolymer during the formation of annuli was believed to cause this high degree of alignment. This motivated us to study the surface structure of cylinder-forming PS-*b*-PMMA diblock copolymer thin films on corrugated silicon surface where it would be possible to cause flow and confinement of the diblock copolymer in a controlled manner, independent of the spontaneous formation of dewetted annuli.

In the present paper we examine the surface structure of PS-*b*-PMMA diblock copolymer thin films on silicon nitride gratings using atomic force microscopy (AFM). The dependence of the surface structure on the thickness of the film[4,42−47] has been utilized to generate periodic polymer structures on two different silicon nitride gratings. The most interesting observations in these experiments are (i) the formation of regularly spaced bumps of almost uniform size on the grating crests and (ii) the remarkable degree of alignment exhibited by lying-down cylindrical domains in the troughs of 555 nm deep silicon nitride gratings. The aligned microdomains in the L thick film regions are perpendicularly oriented to the edges of the troughs and have coherence lengths extending from 350 to 750 nm, essentially limited by trough, i.e., channel, width of the underlying substrate.

Experimental Procedure

Asymmetric PS-*b*-PMMA, obtained from Polysciences, Inc. (Warrington, PA), was 74 wt % PS with a molecular weight of 84 000 g/mol and polydispersity of 1.08. The diblock sample was Soxhlet extracted with cyclohexane to remove excess PS homopolymer. Silicon nitride gratings bought from K-Tek International, Inc., were used as substrates. They were cleaned with trichloroethylene, hot toluene, acetone, and methanol (in this order) using an ultrasonic cleaner. Then, the substrates were kept submerged in methanol until thin films of diblock copolymer were deposited onto these gratings by direct spin-coating from a toluene solution. The same cleaning procedure was followed to recondition previously used gratings. Two different gratings of depths 115 and 555 nm, each with a period of 3 μm, were used in these experiments. The samples were spin-cast using 2% (w/w) to 2.5% (w/w) diblock/toluene solutions at 3500 rpm for 1 min. A drop size of 5 μL (using a micropipet) of polymer solution was used to prepare thin film samples on 555 nm deep gratings. For samples prepared on flat silicon nitride substrates and 115 nm deep gratings, a normal glass pipet having a droplet size in the range 20−40 μL was used. Subsequent thermal annealing of the samples was carried out at 523 K under an argon atmosphere. Annealing was achieved by a transient ramp up rate of 5 K/min from room temperature and quenched back to room temperature with a cooling rate of 20 K/min. AFM measurements were then conducted to examine the resulting microphase separation behavior of diblock copolymer thin films. Tapping mode AFM was performed with silicon Nanoprobe SPM tips (TESP, resonance frequency ~ 320 kHz) and a contact mode AFM with silicon nitride Nanoprobe SPM tips, NP-20, using a Nanoscope IIIa, Digital Instruments Multimode SPM.

Except for the thin film sample shown in Figure 5, the presence of featureless $L/2$ thick region (21 nm thick; Figures 3 and 4) or the bare silicon nitride surface (Figures 6 and 8) on the crest gives us a reference to find thickness of the films in the trough and on the crest regions. The sample in Figure 5 has the crest region completely covered by a uniform film with (just) lying-down cylinders on it. Therefore, the thickness of the film on the crest can be L, $2L$, or any integer multiple of L, i.e., nL. When the edge of the grating lines (on this sample) was scanned with AFM, the dewetted film with bare silicon nitride surface was observed on the crest regions. This bare silicon nitride surface, again, gave us a reference to calculate the thickness of the film on the crest. Then, the thickness of the film in the troughs could also be calculated (knowing that the corrugation of the grating without a polymer film equals 115 nm). They were measured to be L thick on the crest and $5L/2$ thick in the trough.

Results and Discussion

In this paper, we discuss the behavior of PS-*b*-PMMA diblock copolymer thin films on two different silicon nitride square gratings having 3 μm period and depths of 115 and 555 nm. We also compare the surface structure of thin films deposited on such gratings with those grown on flat silicon nitride substrates. To obtain

films of uniform thickness on gratings, they are usually first prepared on flat substrates and then transferred onto the gratings.[40,41] However, in our experiments we use spin coating directly on the grating, and because of the corrugation, we obtain nonuniform films. Thermal annealing of the samples leads to clearly resolved height quantization due to the wetting properties and mutual incompatibilities of the two blocks in the copolymer.[3] Asymmetric wetting occurs when one component of a given diblock wets the substrate interface while the other component wets the air interface; the resulting polymer film is referred to as odd number quantized. The film thickness, then, corresponds to odd multiples of $L/2$, that is, $(2n + 1)L/2$, where n is an integer and L equals 43 nm ($\sqrt{3}/2$ multiplied by 50 nm, where lattice period corresponding to the center-to-center distance between nearest-neighbor cylinders is 50 nm) for PS-*b*-PMMA of molecular weight 84 000 g/mol. However, in the case of symmetric wetting, when the same block wets both the substrate and air interfaces, the height quantized film thickness corresponds to even multiples of $L/2$, that is, $2nL/2$. PMMA prefers to wet the silicon nitride/polymer interface due to its lower wetting energy whereas PS exhibits an affinity for the polymer/air interface. The surface tension difference between PS and PMMA is small; therefore, for L thick films, both components of the diblock are present at the air/polymer interface. This generates the characteristic "fingerprint pattern" of lying down cylinders in nL thick regions.[4]

Figure 1a shows the topographic AFM image of islands and holes, which are formed when a thin film of PS-*b*-PMMA of average thickness 50 nm is prepared on a flat silicon nitride substrate. The sample, prepared by spin-coating at 3500 rpm for 1 min, was annealed at 523 K for 12 h.The islands here correspond to $3L/2$ thick film regions whereas holes correspond to L thick film regions. The phase image of Figure 1b shows the morphology of standing-up cylinders in $3L/2$ thick regions, while the morphology of L thick regions exhibits lying-down cylinders, that is, half cylinders parallel to the substrate with both PS and PMMA appearing at the polymer/air interface. The morphology of cylinders depends on the film thickness, and the surface structure can evolve further if this sample is annealed for a longer duration.[4,42,47] Recent self-consistent-field arguments also predict the morphological transitions of copolymers as a function of film thickness, and "hybrid" or "mixed orientation" morphology of cylinders can also be observed.[42,45,47] In this paper, the cylindrical block copolymer domains which appear as hexagonally packed circles on the surface (Figure 1b) will be referred to as "standing-up cylinders". As mentioned before, PMMA prefers to wet the silicon nitride/polymer interface, and for $L/2$ thickness, a monolayer of diblock copolymer covers the substrate. Therefore, the surface of the $L/2$ thick film is featureless. If additional layers of L thick film are deposited over this $L/2$ thick film, the film thickness, then, corresponds to odd multiples of $L/2$, that is, $(2n + 1)L/2$. It is believed that these hexagonally packed cylindrical domains on the surface for odd-number-quantized film are perpendicular to the substrate plane in the near-free-surface region only, and they do not traverse the film completely.[42,47] Previously, combined AFM and transmission electron microscopy (TEM) imaging at the same film location was used to access the local film morphology in L thick film regions, resulting in the assignment of higher regions (shown as lighter shading in Figure 1b), as observed in topographic and phase AFM images, to PMMA-rich regions

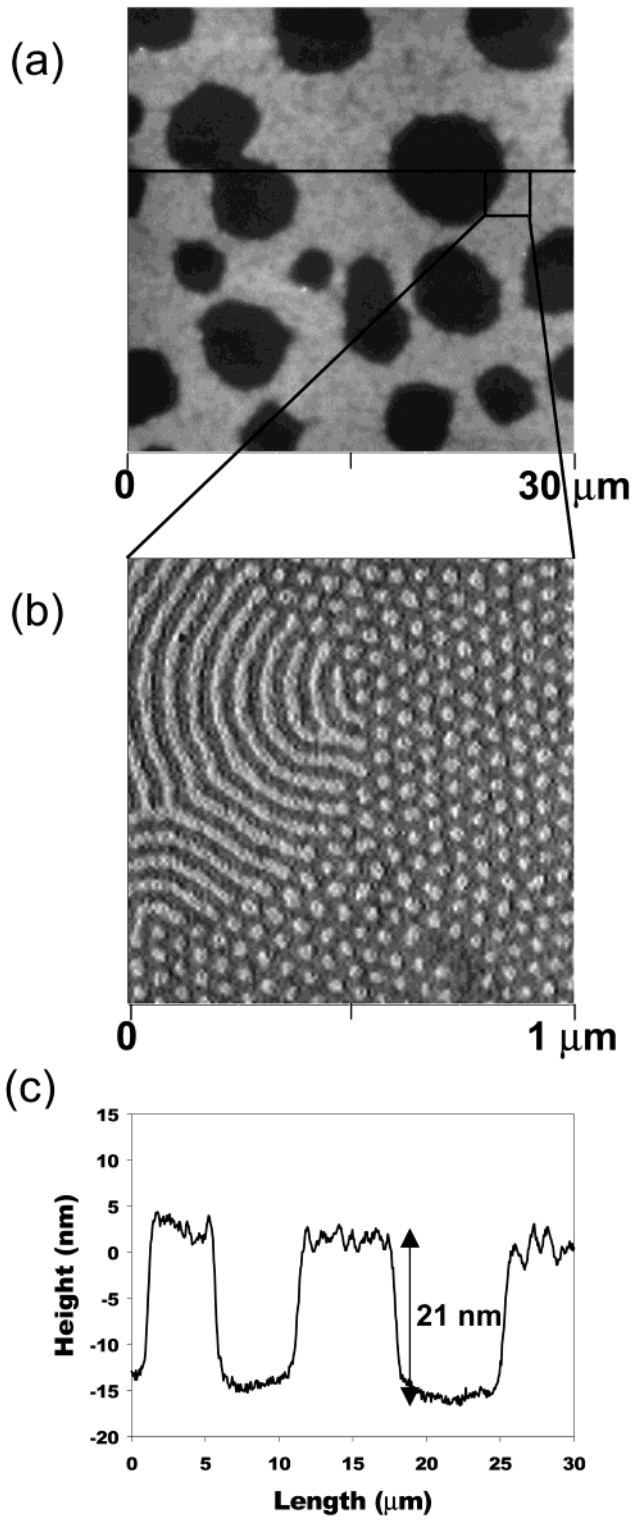

Figure 1. (a) Topographic AFM image, 30 μm × 30 μm, of PS-*b*-PMMA thin film on a flat silicon nitride substrate obtained by tapping mode AFM. The sample is prepared by spin-coating at 3500 rpm for 1 min. Islands (lighter shading) and holes (darker shading) are formed when the film is annealed at 523 K for 12 h. The islands correspond to $3L/2$ thick regions (64.5 nm thick), and holes correspond to L thick regions (43 nm thick). (b) Phase tapping mode AFM image, 1 μm × 1 μm, of the inset in (a). The holes have lying-down cylindrical domains whereas islands have standing-up cylindrical domains. (c) Height profile of the inserted line in (a). The height difference from the island to hole is 21 nm.

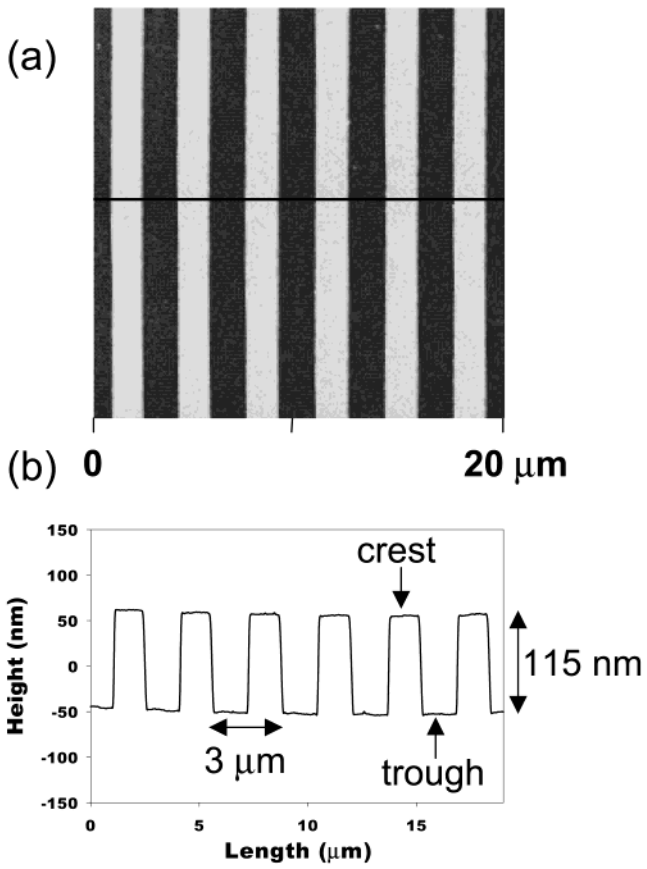

Figure 2. (a) Contact mode AFM image, 20 μm × 20 μm, of a bare silicon nitride grating. (b) Height profile of the inserted line in (a). This grating has a periodicity of 3 μm and depth of 115 nm. The crests and troughs have equal width of 1.5 μm.

and lower regions (shown as darker shading in Figure 1b) to PS-rich regions.[4] The repeat spacing between the cylinders is 50 nm. The difference in height from islands to holes, as shown in the section analysis in Figure 1c, is $L/2$ or ∼21 nm.

A topographic AFM image showing the structure of a bare silicon nitride grating with its corresponding height profile is shown in Figure 2. This image was obtained by scanning the grating of depth 115 nm and periodicity 3 μm. Another grating used in these experiments has the same basic "square-wave" structure. From the height profile in Figure 2b we can observe that crests and troughs have sharp edges and widths of 1.5 μm.

When the sample preparation conditions similar to that used for flat silicon nitride substrate in Figure 1 were performed on 115 nm deep silicon nitride gratings, the polymer film (when annealed at 523 K for 24 h), instead of forming islands and holes, formed continuous strips of films of different thickness on the crests and in the troughs. The images shown in Figure 3 have L thick and $L/2$ thick films on the crests and $2L$ thick film in the troughs. The featureless region of $L/2$ thick film, which is ∼21 nm thick, on the crest helped us to determine the thickness of the film on the crests and in the troughs. Even when imaging large scan regions on this sample, there seem to be no breaks in the films of various thicknesses. The trough region, observed closely in Figure 3b, has standing-up cylinders along the edges of the troughs. From the section profile in Figure 3c, it is clear that this region has film of continuously increasing thickness until it reaches the

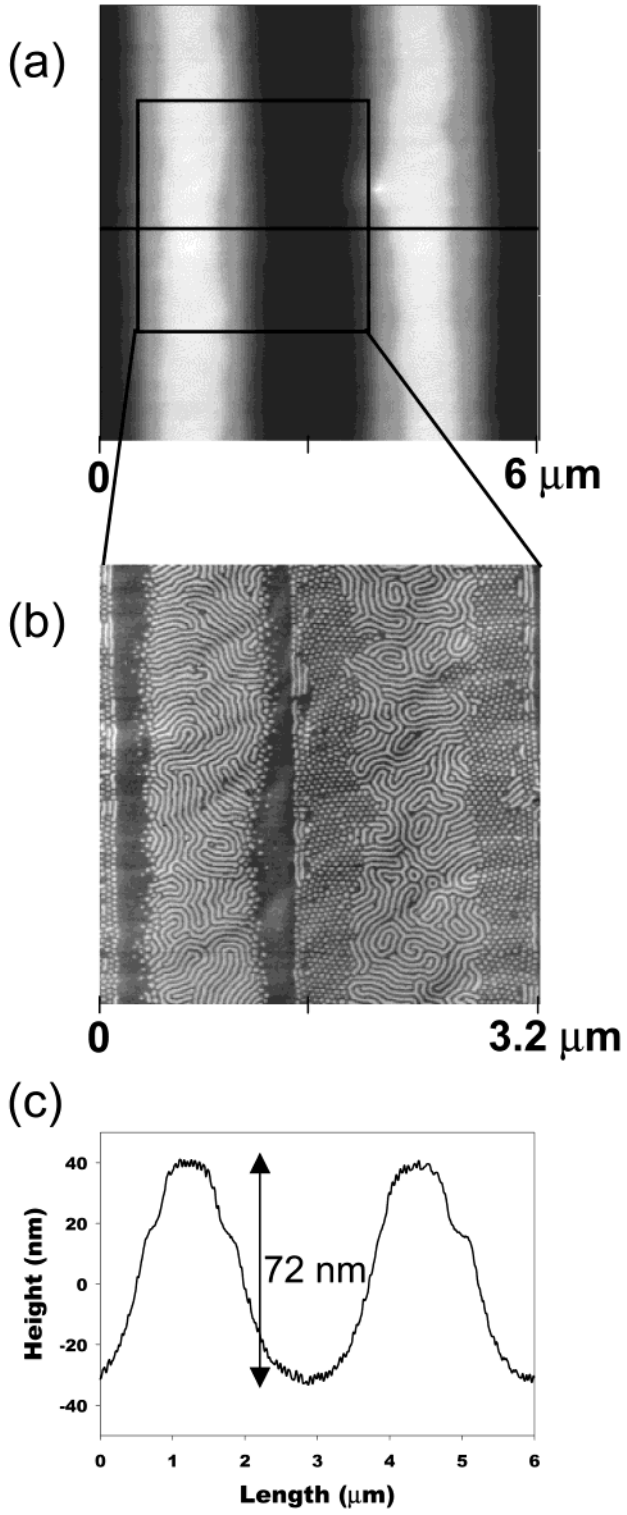

Figure 3. (a) Topographic AFM image, 6 μm × 6 μm, of PS-*b*-PMMA thin film on a silicon nitride grating (periodicity 3 μm, depth 115 nm) obtained by tapping mode AFM. The sample is spin-cast at 3500 rpm for 1 min and then annealed at 523 K for 24 h. The crest has L thick and $L/2$ thick regions. The trough has $2L$ thick film in the center. (b) Phase tapping mode AFM image, 3.2 μm × 3.2 μm, of the inset in (a) showing one crest (to the left) and one trough (to the right). The $L/2$ thick film on the crest is featureless. (c) Height profile of the inserted line in (a). The height difference from the L thick region on the crest to the center of the trough is 72 nm.

crest. The width of the L thick strip on the crest depends on the number of hours this sample is annealed, and we have observed the gradual decrease in width as more

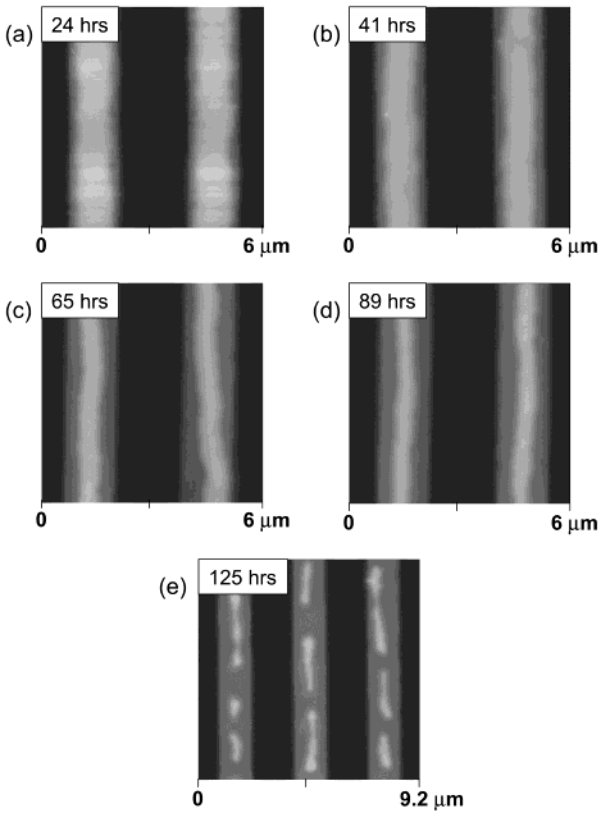

Figure 4. Sequential topographic AFM images obtained in tapping mode of a thin film of PS-*b*-PMMA prepared on a silicon nitride grating (periodicity 3 μm, depth 115 nm) and annealed at 523 K for a total time of (a) 24 h (6 μm × 6 μm), (b) 41 h (6 μm × 6 μm), (c) 65 h (6 μm × 6 μm), (d) 89 h (6 μm × 6 μm), and (e) 125 h (9.2 μm × 9.2 μm).

and more polymer, being mobile above its glass transition temperature, flows into the troughs during annealing. Eventually, when the *L* thick strip becomes very narrow, it starts to fragment (Figure 4). Then, an increase in the thickness of the film in the troughs causes a significant change in cylinder morphology. More standing-up cylinders, indicative of a "hybrid" or "mixed orientation" morphology,[42,45,47] were observed in the center of the trough regions, which were completely absent for thinner film structure. This provides a simple technique to observe a gradual change in surface morphology as a function of film thickness.

The thickness of the film in the trough regions is highly sensitive to both the concentration of the polymer solution and the spinning speed at which the sample is spin-cast. Either by decreasing the spinning speed or by increasing the concentration of the polymer solution to more than 2%, we can fill more polymer in the troughs to generate thicker film in the trough regions. Figure 5a shows the topographic image of one such sample, deposited on a 115 nm deep grating, which has *L* thick film on the crests and 5*L*/2 thick film in the troughs. This explains the height difference of 51 nm from the crest to the trough as shown in the height profile in Figure 5c. This simple method can generate micron-scale periodic structures with standing-up cylinders in the troughs (5*L*/2 thick film) and lying-down cylinders on the crests (*L* thick film) present over the entire sample (Figure 5b). During these experiments, we have also observed that the coverage of polymer on the crest after spin-coating depends on whether the polymer drop is placed on the substrate before or after

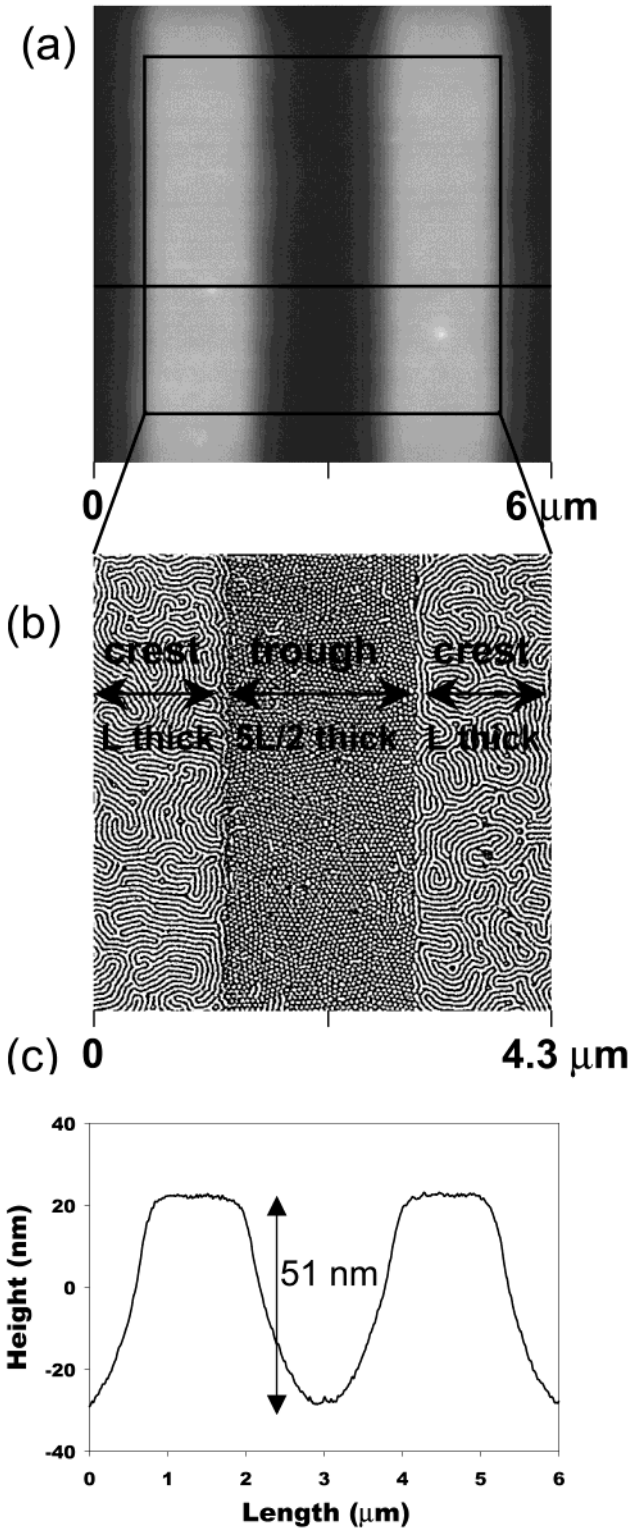

Figure 5. (a) Topographic AFM image, 6 μm × 6 μm, of PS-*b*-PMMA thin film on a silicon nitride grating (periodicity 3 μm, depth 115 nm) obtained by tapping mode AFM. The sample, prepared by spin-coating at 3500 rpm for 1 min using ~2.5% polymer solution, is annealed at 523 K for 6 h. The crest has *L* thick film and trough has 5*L*/2 thick film. (b) Phase tapping mode AFM image, 4.3 μm × 4.3 μm, of the inset in (a) showing two crests and one trough. The crest with *L* thick film has lying-down cylindrical domains, and the trough with 5*L*/2 thick film has standing-up cylindrical domains. (c) Height profile of the inserted line in (a). The height difference from the crest to the trough is 51 nm.

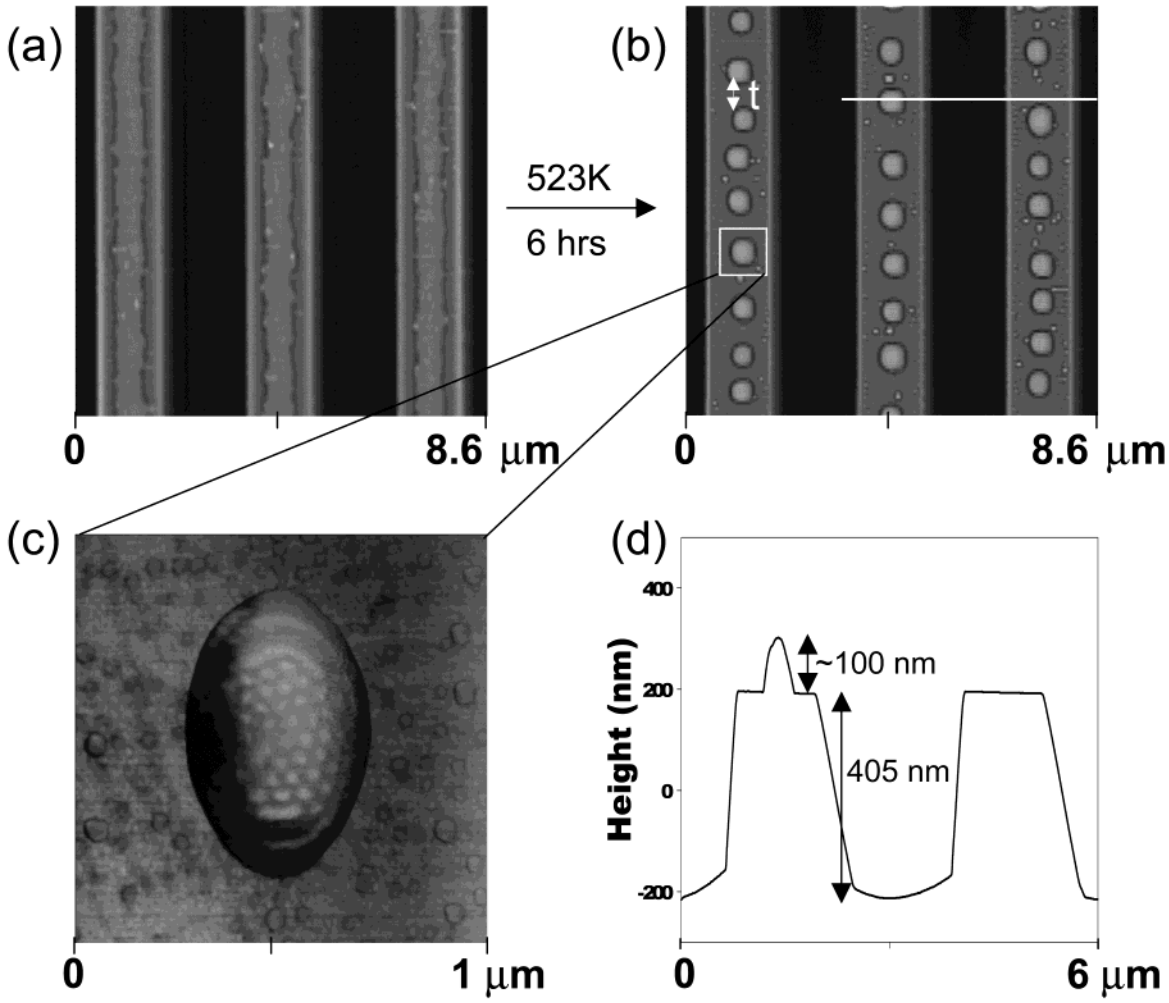

Figure 6. Contact mode topographic AFM images, 8.6 μm × 8.6 μm, of a PS-*b*-PMMA thin film sample prepared by spin-coating at 3500 rpm for 1 min with a drop size of 5 μL on a silicon nitride grating (periodicity 3 μm, depth 555 nm) using 2.5% polymer solution. (a) Before the sample is annealed. (b) After the sample is annealed at 523 K for 6 h. (c) Phase tapping mode AFM image, 1 μm × 1 μm, of the inset in (b) showing phase-separated microstructure within a bump. (d) Height profile of the white scan line shown in (b). The bumps have the average height of 100 nm (~5L/2) at their center. The corrugation from the bare silicon nitride surface on the crest to the center of the trough is 405 nm.

spinning. For polymer concentrations of ~2.5%, when the sample is prepared by placing the drop on the substrate while spinning, we find that instead of forming just L thick film on the crest, it forms a thin continuous strip of 3L/2 thick film located on the middle region of the crest.

We have also done studies of polymer thin films spin-cast on 555 nm deep silicon nitride gratings. The lower concentration of the polymer solution (2−2.5%) and the depth of the grating being much higher than L causes the film to dewet on the crests, although still forming a uniform film in the troughs. The sample prepared with 2.5% polymer solution forms a narrow dewetted film on the crest, which breaks into regularly spaced bumps of almost uniform diameter when the sample is annealed at 523 K for 6 h (Figure 6). The bumps are 90−120 nm in height at the center, and the corrugation from the bare silicon nitride surface on the crest to the thin film in the middle of the trough is 405 nm (Figure 6d). Therefore, the film is 7L/2 (555 − 7 × 43/2 = 404.5) thick in the center of the troughs for this sample. Before annealing the dewetted film on the crest has no fine structure whereas the bumps formed after annealing have microstructure of standing-up cylinders (Figure 6c). The separation (t as shown in Figure 6b) and diameter of the bumps were measured at different regions on one such sample, and the distribution of spacing between the bumps and their diameters are shown in parts b and a of Figure 7, respectively. The average spacing is 387 nm, and the average diameter is 330 nm. These values remain relatively constant when the annealing time is increased by several hours. We have also observed that the diameter distribution and bump spacing distribution do not change from one sample to another prepared under the same conditions.

Spontaneous Cylinder Alignment on Gratings. When a thin film sample is prepared on these gratings using a lower concentration (2%) of the polymer solution, the coverage of polymer and the resulting surface structure are very different than those discussed in previous sections of this paper. Figure 8 shows the topographic structure of the thin film sample on a 555 nm deep grating before and after annealing when prepared with a 2% polymer solution. The sample was annealed at 523 K for 6 h. The thin film on the crest, which is dewetted before annealing, forms polymer fragments instead of regularly spaced bumps after annealing.

The most interesting feature of these studies on this grating is the structure of nanodomains in the trough

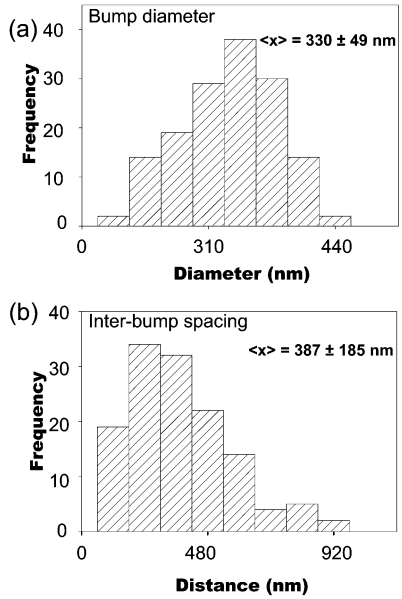

Figure 7. Distribution of (a) bump diameter and (b) inter-bump spacing on the crests when a PS-*b*-PMMA thin film is prepared on a silicon nitride grating (periodicity 3 μm, depth 555 nm). The mean diameter and mean spacing are 330 and 387 nm, respectively.

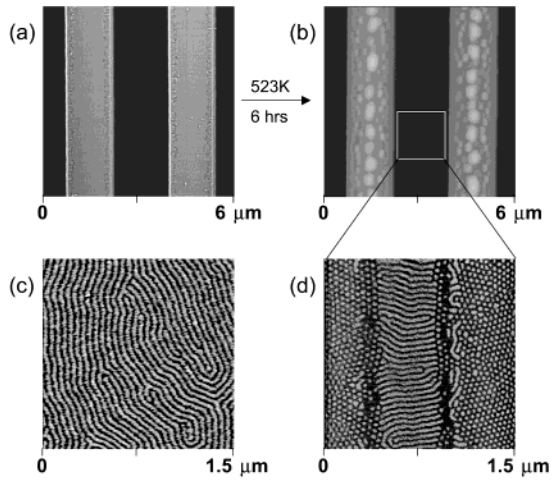

Figure 8. Contact mode topographic AFM images of a PS-*b*-PMMA thin film sample prepared by spin-coating at 3500 rpm for 1 min with a drop size of 5 μL on a silicon nitride grating (periodicity 3 μm, depth 555 nm) using 2% polymer solution. (a) Before the sample is annealed (6 μm × 6 μm). (b) After the sample is annealed at 523 K for 6 h (6 μm × 6 μm). (c) Phase tapping mode AFM image, 1.5 μm × 1.5 μm, of lying-down cylindrical domains in the *L* thick region when a thin film of PS-*b*-PMMA is prepared on a flat silicon nitride substrate; no alignment is present with the flat substrate. (d) Phase tapping mode AFM image, 1.5 μm × 1.5 μm, of the inset in (b). Note the formation of lying-down cylindrical domains which are aligned perpendicular to the grating lines.

regions. When the film is *L* thick in the center of the troughs, the lying-down cylinders show a high degree of alignment perpendicular to the grating lines as shown in the phase image of tapping mode AFM in Figure 8d. To compare, Figure 8c shows the characteristic fingerprint pattern of unaligned lying-down cylinders in *L* thick regions on a normal sample prepared on a flat silicon nitride substrate. The *L* thick region in the troughs is confined between thicker film regions located along the edges of the troughs; these thicker regions only have standing-up cylinders. The alignment of

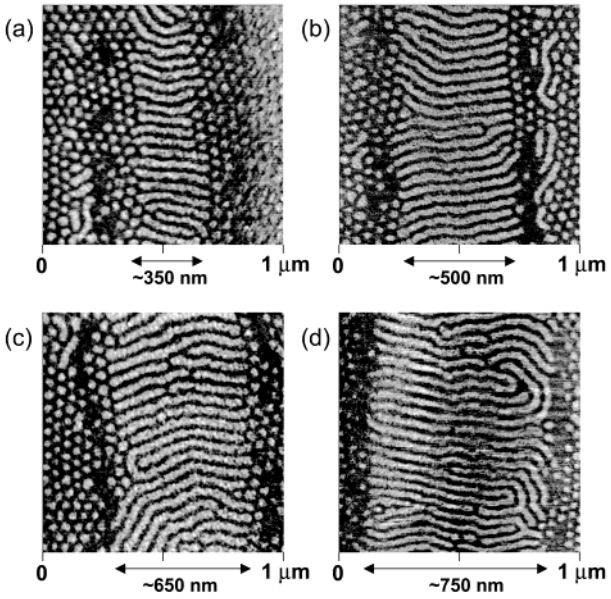

Figure 9. (a) Phase tapping mode AFM images, 1 μm × 1 μm, of the trough region with aligned *L* thick strip in the center. The width of the *L* thick strip for different samples is (a) ~350, (b) ~500, (c) ~650, and (d) ~750 nm. These thin film samples of PS-*b*-PMMA are prepared on silicon nitride gratings with a periodicity of 3 μm and depth of 555 nm.

nanodomains is present throughout the sample and is reproducible. The width of the *L* thick strip in the troughs depends critically on the amount of polymer deposited in the troughs by spin-coating. We have observed different widths of these *L* thick regions in the troughs (Figure 9), varying from 350 to 750 nm, when there is a slight change in the sample preparation conditions. Studies to understand how to control precisely this width are in progress.

The thickness of the film in the troughs is very sensitive to the concentration of the polymer solution, and we have observed that 2% solution is better than 2.5% for consistently obtaining *L* thick films in the center of the troughs. This affects the quality of bumps on the crest as mentioned before.

Proposed Alignment Mechanism. We believe that the flow of the polymer when it is annealed above its glass transition temperature, T_g, combined with capillary action induces this high degree of alignment in the trough regions. The walls of the troughs are not wetted completely when the sample is initially prepared by spin-coating. When the polymer becomes mobile above T_g, the system can lower its surface energy if diblock copolymer wets the bare silicon nitride along the walls. We have observed when a thin film sample is prepared on a 555 nm deep grating using 2% polymer solution that the film does not wet the crest completely (Figure 8a) and that a film thicker than *L* is obtained in the trough regions. The thin dewetted film on the crest observed before annealing is 5−6 nm thick, which forms polymer fragments after the sample is annealed (Figure 8b). In the trough regions, the flow of the polymer due to capillary action along the walls of the troughs induces a flow of polymer from the center of the troughs to its edges. This causes a decrease in the thickness of the film at the center of the troughs, and when the thickness equals *L*, the lying-down cylinders align along the direction of polymer flow, i.e., perpendicular to the grating lines.

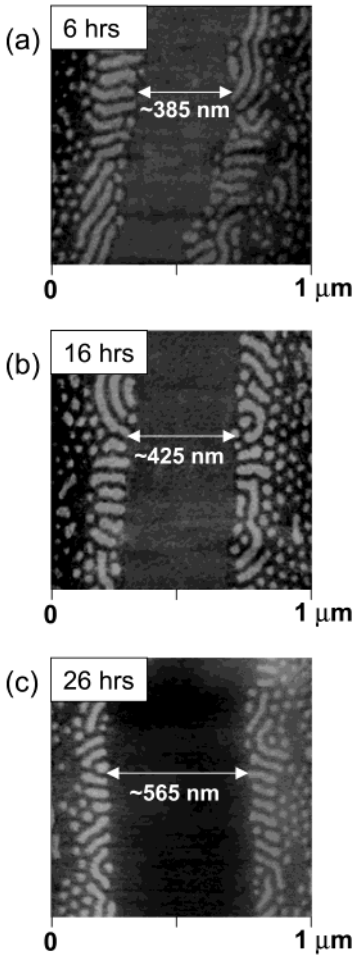

Figure 10. Sequential phase tapping mode AFM images, 1 μm × 1 μm, of a thin film sample of PS-*b*-PMMA prepared on a silicon nitride grating (periodicity 3 μm, depth 555 nm) using low polymer concentration (<2%) and annealed at 523 K for a total time of (a) 6, (b) 16, and (c) 26 h. Note the systematic increase in width of the *L*/2 thick strip in the troughs as a function of annealing time.

We have conducted an experiment where we obtained *L*/2 thick film in the center of the troughs. The time evolution of the width of *L*/2 thick film is observed as a function of annealing time. The increase in width as shown in Figure 10 shows that polymer flows from the center to the edges of the troughs. In another experiment, we obtained aligned *L* thick film in the troughs with several defects or standing-up cylinders at the center, which are due to the film being thinner than *L* at the center (Figure 11a). When this sample was annealed at 523 K for an additional 10 h, the trough regions undergo a dramatic change with the *L* thick film decreasing in thickness to *L*/2 at the center. The featureless region shown in Figure 11b corresponds to *L*/2 thickness. This again is due to polymer flowing from the center to the edges of the troughs. These early results support the proposed mechanism for alignment. We now have the capability to scan the sample at high temperatures in controlled environments using high-temperature AFM. In-situ real-time experiments are in progress to observe this alignment phenomenon on silicon nitride gratings at high temperatures.

Conclusion

Using silicon nitride gratings as substrates for thin diblock copolymer film samples provides a simple method

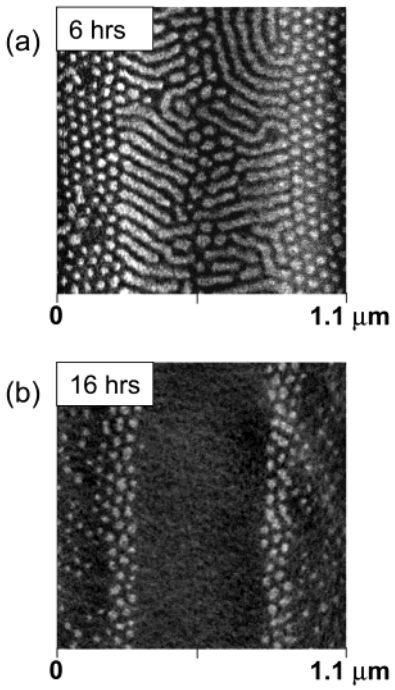

Figure 11. Sequential phase tapping mode AFM images, 1.1 μm × 1.1 μm, of the trough regions in a thin film sample of PS-*b*-PMMA prepared on a silicon nitride grating (periodicity 3 μm, depth 555 nm) using 2% polymer concentration and annealed at 523 K for a total time of (a) 6 h (*L* thick with alignment) and (b) 16 h (*L*/2 thick; no surface features).

to generate controlled periodic structures on the surface. With the gratings of depth 115 nm, we can easily generate micron-scale periodic structures with standing-up cylinders in troughs and lying-down cylinders on the crests. Previously, the alignment of lying-down cylindrical domains in asymmetric PS-*b*-PMMA thin films has been obtained by (i) the application of electric field in which thin films were spin-coated onto silicon nitride substrates patterned with planar electrodes. The cylindrical domains were observed to align parallel to the electric field lines, after the samples were annealed at 523 K in an argon atmosphere for 24 h. This technique, causing alignment between two closely spaced electrodes, could only be used to locally control the domain orientation on micrometer-length scales[19] and (ii) the formation of annuli due to polymer dewetting on silicon oxide substrates, as previously discussed.[18]

The method described in this paper can be used to reproducibly generate aligned nanostructures consisting of lying-down cylindrical domains in *L* thick regions in the troughs of selected silicon nitride gratings, present throughout the sample. Alignment occurs in a controlled fashion without the aid of an external orientation field. We have also observed the formation of regularly spaced bumps of essentially uniform size on the crests of the 555 nm deep gratings. The average diameter and spacing between the bumps are 330 and 387 nm, respectively. Further experiments to delineate the mechanism of bump formation and bump nanostructure are clearly warranted.

The spacing of the aligned and orientationally ordered cylinders in troughs can be tuned by varying easily controlled experimental parameters, such as the molecular weight or volume fraction of the diblock copolymer. In all of the experiments herein discussed, we have used gratings consisting of 50% troughs/50% crests with

equal widths of 1.5 μm. Alignment occurs only in the trough region corresponding to half the total sample area. Note, however, that the ratio of trough width to crest width covered areas can be altered against or in favor of the percentage of surface area encompassed by trough regions; this can be easily achieved using substrates with different patterns. This gives an experimental route to fabricate aligned polymers over a large fraction of the available surface area. Alternatively, the utilization of narrower or wider square-wave gratings, or even variable width patterns, gives a facile route to complex grating structures. Experiments using different grating presentations are currently underway. Such aligned nanodomains can be used, for example, to prepare nanowires for electron transport or magnetic storage by selective decoration of individual diblock components with conductive or magnetic species, including nanoparticles.

Acknowledgment. We gratefully acknowledge Professor Thomas Witten and Vladimir Belyi for useful discussions. This work was primarily supported by the NSF-Materials Research Science and Engineering Center at The University of Chicago, DMR-9808595. Further support for instrumentation development is also acknowledged from the Air Force Office of Scientific Research.

References and Notes

(1) Bates, F. S.; Fredrickson, G. H. *Annu. Rev. Phys. Chem.* **1990**, *41*, 525.
(2) Carvalho, B. L.; Thomas, E. L. *Phys. Rev. Lett.* **1994**, *73*, 3321.
(3) Coulon, G.; Collin, B.; Ausserre, D.; Chatenay, D.; Russell, T. P. *J. Phys. (Paris)* **1990**, *51*, 2801.
(4) Morkved, T. L.; Lopes, W. A.; Hahm, J.; Sibener, S. J.; Jaeger, H. M. *Polymer* **1998**, *39*, 3871.
(5) Mansky, P.; Chaikin, P. M.; Thomas, E. L. *J. Mater. Sci.* **1995**, *30*, 1987.
(6) Harrison, C.; Park, M.; Chaikin, P. M.; Register, R. A.; Adamson, D. H. *J. Vac. Sci. Technol. B* **1998**, *16*, 544.
(7) Zehner, R. W.; Lopes, W. A.; Morkved, T. L.; Jaeger, H. M.; Sita, L. R. *Langmuir* **1998**, *14*, 241.
(8) Hahm, J.; Lopes, W. A.; Jaeger, H. M.; Sibener, S. J. *J. Chem. Phys.* **1998**, *109*, 10111.
(9) Huang, E.; Mansky, P.; Russell, T. P.; Harrison, C.; Chaikin, P. M.; Register, R. A.; Hawker, C. J.; Mays, J. *Macromolecules* **2000**, *33*, 80.
(10) Harrison, C.; Park, M.; Chaikin, P. M.; Register, R. A.; Amundson, D. H.; Yao, N. *Polymer* **1998**, *39*, 2733.
(11) Hahm, J.; Sibener, S. J. *J. Chem. Phys.* **2001**, *114*, 4730.
(12) Harrison, C.; Adamson, D. H.; Cheng, Z.; Sebastian, J. M.; Sethuraman, S.; Huse, D. A.; Register, R. A.; Chaikin, P. M. *Science* **2000**, *290*, 1558.
(13) Amundson, K.; Helfand, E.; Davis, D. D.; Quan, X.; Patel, S. S.; Smith, S. D. *Macromolecules* **1991**, *24*, 6546.
(14) Hamley, I. W. *J. Phys.: Condens. Matter* **2001**, *13*, R643.
(15) Amundson, K.; Helfand, E.; Quan, X.; Hudson, S. D.; Smith, S. D. *Macromolecules* **1994**, *27*, 6559.
(16) Bodycomb, J.; Funaki, Y.; Kimishima, K.; Hashimoto, T. *Macromolecules* **1999**, *32*, 2075.
(17) Boker, A.; Knoll, A.; Elbs, H.; Abetz, V.; Muller, A. H. E.; Krausch, G. *Macromolecules* **2002**, *35*, 1319.
(18) Hahm, J.; Sibener, S. J. *Langmuir* **2000**, *16*, 4766.
(19) Morkved, T. L.; Lu, M.; Urbas, A. M.; Ehrichs, E. E.; Jaeger, H. M. *Science* **1996**, *273*, 931.
(20) Thurn-Albrecht, T.; Schotter, J.; Kastle, G. A.; Emley, N.; Shibauchi, T.; Krusin-Elbaum, L.; Guarini, K.; Black, C. T.; Tuominen, M. T.; Russell, T. P. *Science* **2000**, *290*, 2126.
(21) Fukunaga, K.; Elbs, H.; Magerle, R.; Krausch, G. *Macromolecules* **2000**, *33*, 947.
(22) Coulon, G.; Russell, T. P.; Deline, V. R.; Green, P. F. *Macromolecules* **1989**, *22*, 2581.
(23) Huang, E.; Russell, T. P.; Harrison, C.; Chaikin, P. M.; Register, R. A.; Hawker, C. J.; Mays, J. *Macromolecules* **1998**, *31*, 7640.
(24) Thurn-Albrecht, T.; Steiner, R.; DeRouchey, J.; Stafford, C. M.; Huang, E.; Bal, M.; Tuominen, M.; Hawker, C. J.; Russell, T. P. *Adv. Mater.* **2000**, *12*, 787.
(25) Peters, R. D.; Yang, X. M.; Kim, T. K.; Sohn, B. H.; Nealey, P. F. *Langmuir* **2000**, *16*, 4625.
(26) Balazs, A. C.; Huang, K. L.; McElwain, P.; Brady, J. E. *Macromolecules* **1991**, *24*, 714.
(27) Chakrabarti, A.; Chen, H. *J. Polym. Sci., Part B* **1998**, *36*, 3127.
(28) Petera, D.; Muthukumar, M. *J. Chem. Phys.* **1998**, *109*, 5101.
(29) Pereira, G. G.; Williams, D. R. M. *Langmuir* **1999**, *15*, 2125.
(30) Fasolka, M. J.; Mayes, A. M. *Annu. Rev. Mater. Res.* **2001**, *31*, 323.
(31) Rockford, L.; Liu, Y.; Mansky, P.; Russell, T. P.; Yoon, M.; Mochrie, S. G. J. *Phys. Rev. Lett.* **1999**, *82*, 2602.
(32) Heier, J.; Kramer, E. J.; Walheim, S.; Krausch, G. *Macromolecules* **1997**, *30*, 6610.
(33) Yang, X. M.; Peters, R. D.; Nealey, P. F.; Solak, H. H.; Cerrina, F. *Macromolecules* **2000**, *33*, 9575.
(34) Podariu, I.; Chakrabarti, A. *J. Chem. Phys.* **2000**, *113*, 6423.
(35) Turner, M. S.; Joanny, J.-F. *Macromolecules* **1992**, *25*, 6681.
(36) Segalman, R. A.; Yokoyama, H.; Kramer, E. J. *Adv. Mater.* **2001**, *13*, 1152.
(37) Park, C.; Cheng, J. Y.; Fasolka, M. J.; Mayes, A. M.; Ross, C. A.; Thomas, E. L.; Rosa, C. D. *Appl. Phys. Lett.* **2001**, *79*, 848.
(38) Heier, J.; Genzer, J.; Kramer, E. J.; Bates, F. S.; Walheim, S.; Krausch, G. *J. Chem. Phys.* **1999**, *111*, 11101.
(39) Fasolka, M. J.; Harris, D. J.; Mayes, A. M.; Yoon, M.; Mochrie, S. G. J. *Phys. Rev. Lett.* **1997**, *79*, 3018.
(40) Li, Z.; Qu, S.; Rafailovich, M. H.; Sokolov, J.; Tolan, M.; Turner, M. S.; Wang, J.; Schwarz, S. A.; Lorenz, H.; Kotthaus, J. P. *Macromolecules* **1997**, *30*, 8410.
(41) Li, Z.; Tolan, M.; Hohr, D. K.; Qu, S.; Sokolov, J.; Rafailovich, M. H.; Lorenz, H.; Kotthaus, J. P.; Wang, J.; Sinha, S. K.; Gibaud, A. *Macromolecules* **1998**, *31*, 1915.
(42) Kim, H.; Russell, T. P. *J. Polym. Sci., Part B* **2001**, *39*, 663.
(43) Wang, Q.; Nealy, P. F.; de Pablo, J. J. *Macromolecules* **2001**, *34*, 3458.
(44) Suh, K. Y.; Kim, Y. S.; Lee, H. H. *J. Chem. Phys.* **1998**, *108*, 1253.
(45) Fasolka, M. J.; Banerjee, P.; Mayes, A. M.; Pickett, G.; Balazs, A. C. *Macromolecules* **2000**, *33*, 5702.
(46) Huinink, H. P.; Brokken-Zijp, J. C. M.; van Dijk, M. A.; Sevink, G. J. A. *J. Chem. Phys.* **2000**, *112*, 2452.
(47) Knoll, A.; Horvat, A.; Lyakhova, K. S.; Krausch, G.; Sevink, G. J. A.; Zvelindovsky, A. V.; Magerle, R. *Phys. Rev. Lett.* **2002**, *89*, 035501.

MA020674P